

Active quantum matter from monitored pure-state dynamics

Jacob F. Steiner,¹ Felix von Oppen,² and Reinhold Egger³

¹*Department of Physics and Institute for Quantum Information and Matter,
California Institute of Technology, Pasadena, California 91125, USA*

²*Dahlem Center for Complex Quantum Systems, Fachbereich Physik, and Halle-Berlin-Regensburg
Cluster of Excellence CCE, Freie Universität Berlin, 14195 Berlin, Germany*

³*Institut für Theoretische Physik, Heinrich-Heine-Universität, D-40225 Düsseldorf, Germany*

Quantum many-body systems coupled to out-of-equilibrium reservoirs can behave as active matter and exhibit signs of flocking. However, the resulting steady states are highly mixed and carry only weak quantum signatures. We show that signatures of active matter also arise in ensembles of pure states undergoing monitored quantum dynamics. We consider a spinful Luttinger liquid subject to measurement processes that shuffle spin-up particles to the left and spin-down particles to the right. For weak monitoring strengths and ferromagnetic spin interactions, we find power-law quantum correlations between spin current and charge density, which we identify as a hallmark of active quantum matter. The monitoring plays a dual role, generating the quantum active correlations for weak strengths while driving a Berezinskii-Kosterlitz-Thouless (BKT) phase transition to a short-range correlated state at larger strengths.

Introduction.—Classical active matter has attracted enormous attention due to its rich phenomenology and broad range of applicability [1–4]. A representative subclass of active matter are interacting assemblies of self-propelled particles which spontaneously align their direction of motion and form a flock [5–10]. The self-propulsion allows these systems to bypass the Mermin-Wagner theorem and exhibit spontaneous breaking of a continuous symmetry in two spatial dimensions [5, 11]. Even one-dimensional (1D) active Ising chains, while not technically long-range ordered, exhibit a transition from a disordered to a phase-separated regime that is characterized by finite-lifetime clusters of particles moving together on a disordered background [6, 7, 12].

It is natural to ask whether and how these phenomena translate to quantum systems. Very recently, first forays into this largely uncharted territory have been undertaken, broadly following two distinct approaches. First, a number of works aimed at establishing minimal structures required to endow a quantum particle with the ability to propel itself. These considered quantum walks [13], classical noise [14–16], or heat-to-motion conversion [17]. Active motion has also been investigated for defects in spin textures [18, 19]. Second, collective effects of interacting self-propelled quantum particles were studied based on nonhermitian Hamiltonian [16, 20] as well as Lindbladian [21] dynamics. The models studied in Refs. [16, 20, 21] are closely related to the active Ising model of Ref. [6], describing spin- $\frac{1}{2}$ particles subject to incoherent directed hopping and spin alignment mechanisms. In particular, Khasseh *et al.* [21] predict signatures of flocking to survive in the presence of sufficiently weak quantum spin-flip processes.

These first steps towards a theory of active quantum matter leave key issues open. If directed motion and alignment are due to incoherent (and hence essentially classical) processes, one expects low-purity mixed states at long times, so that quantum signatures are observable only as transient correlations. Here we pose, and answer

in the affirmative, the question: Can active quantum matter be based solely on the fundamental ingredients of quantum many-body dynamics, namely unitary time evolution and quantum measurements [22, 23]? For a pure initial state and a given measurement trajectory, the system then remains in a pure state at all times.

We study a 1D quantum active model of spin- $\frac{1}{2}$ fermions with ferromagnetic Ising coupling, similar to Ref. [21], but employ only monitored quantum dynamics, i.e., unitary dynamics combined with weak continuous measurements [22]. We design the measurements to generate directed hopping and thus self-propulsion. The measurements allow energy and information exchange between individual particles and the detectors, thereby equipping our model with the defining characteristic of quantum active matter [10]. The resulting pure-state dynamics exhibit features of quantum active motion manifested in quasi-long-range (algebraically decaying) quantum correlations between spin density and charge current. Initially, these correlations grow with increasing monitoring strength or ferromagnetic coupling. In this sense, the system forms an incipient quantum flock.

Importantly, the monitoring plays a dual role. Beyond a critical strength, it drives a transition to a phase in which the correlations between spin density and charge current become short-ranged. This BKT transition [24] between phases with distinct levels of quantum active correlations is directly related to the charge sharpening transition in U(1)-symmetric monitored quantum many-body systems [25–28]. We discuss our monitoring scheme—implemented via nonhermitian jump operators that drive self-propulsion—and its competition with the unitary dynamics within an intuitive lattice model. We use a corresponding bosonized continuum theory, a nonhermitian spinful Luttinger liquid with a sine-Gordon nonlinearity, to gain analytical access to the BKT transition. This builds on recent work on spinless models with monitoring of hermitian operators [29–31].

Lattice models of generic U(1)-symmetric monitored

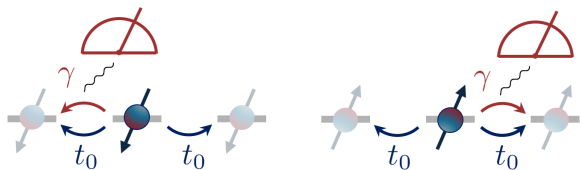


FIG. 1. Cartoon of kinetic processes in the 1D monitored lattice model defined by Eqs. (1)-(3). Spin-independent and bidirectional motion is due to hopping with amplitude t_0 (blue). Spin-dependent unidirectional motion is induced by monitoring with monitoring strength γ (red).

systems [25–28] exhibit a transition between volume- and area-law entangled phases in addition to the charge-sharpening transition [32–42]. Calculations indicate that this entanglement transition occurs at even stronger monitoring within the charge-sharp phase [25–28]. By analogy, we expect the BKT transition to separate two distinct volume-law entangled phases, while the entanglement transition can be viewed as the boundary between quantum and classical active phases.

Lattice model.—We describe the monitored evolution of a 1D chain of spin- $\frac{1}{2}$ fermions $c_{x,\sigma}$ with site index $x \in \mathbb{Z}$ and spin $\sigma \in \{\uparrow, \downarrow\}$ by the stochastic Schrödinger equation [22, 23]

$$i \frac{d}{dt} |\psi_c\rangle = \left\{ H - \frac{i}{2} \sum_{x,\sigma} \left[L_{x,\sigma}^\dagger L_{x,\sigma} - 2W_{x,\sigma} L_{x,\sigma} + W_{x,\sigma}^2 + 2\xi_{x,\sigma} (L_{x,\sigma} - W_{x,\sigma}) \right] \right\} |\psi_c\rangle. \quad (1)$$

The subscript c denotes conditioning on the measurement trajectory. The terms involving $W_{x,\sigma} = \text{Re} \langle \psi_c | L_{x,\sigma} | \psi_c \rangle$ ensure normalization of $|\psi_c\rangle$. The unitary dynamics obey a Hamiltonian H including nearest-neighbor hopping t_0 and ferromagnetic Ising exchange $J_z > 0$,

$$H = \sum_x \left[-t_0 (c_x^\dagger c_{x+1} + \text{h.c.}) - J_z S_x^z S_{x+1}^z \right] + H_{\text{flip}}, \quad (2)$$

where $S_x^z = \frac{1}{2} c_x^\dagger \sigma_3 c_x$ and $c_x = [c_{x,\uparrow}, c_{x,\downarrow}]^\top$. The Pauli matrices $(\sigma_1, \sigma_2, \sigma_3)$ act in spin space. We also allow for spin-nonconserving dynamics through a time-reversal odd Zeeman term, $H_{\text{flip}} = h \sum_x c_x^\dagger \sigma_1 c_x$, or a time-reversal even Rashba spin-orbit coupling, $H_{\text{flip}} = -i\alpha \sum_x c_x^\dagger \sigma_1 c_{x+1} + \text{h.c.}$. The self-propulsion of spin- σ fermions is achieved by monitoring with the nonhermitian jump operators

$$L_{x,\sigma} = \sqrt{\gamma} c_{x+\sigma,\sigma}^\dagger c_{x,\sigma}, \quad (3)$$

with monitoring strength γ . The random sequence of measurement outcomes is encoded by the Gaussian white noise sources $\xi_{x,\sigma}$ with $\xi_{x,\sigma}(t) = 0$ and correlations $\overline{\xi_{x,\sigma}(t) \xi_{x',\sigma'}(t')} = \delta_{x,x'} \delta_{\sigma,\sigma'} \delta(t-t')$, where the overline denotes averaging over the ensemble of measurement

outcomes. We emphasize that for a single measurement trajectory, Eq. (1) preserves purity at all times t .

The kinetic processes of our model are graphically represented in Fig. 1. Spin-independent coherent hopping without preferred direction (amplitude t_0) builds up entanglement. Spin-dependent directional stochastic jumps are induced by monitoring (jump operators in Eq. (3)). This can be realized experimentally, e.g., by exploiting cotunneling in a chain of quantum dots [43] weakly coupled to an auxiliary chain of spin-polarized detector dots whose charge state is monitored, see the Supplemental Material (SM) [44] for details. Our model differs from the one discussed in Ref. [21] even with regard to the Lindblad evolution $\dot{\rho}_1 = \mathcal{L}\rho_1 = -i[H, \rho_1] + \sum (L\rho_1 L^\dagger - \frac{1}{2} \{L^\dagger L, \rho_1\})$ [22, 23, 45] of the ensemble-averaged state $\rho_1 = |\psi_c\rangle\langle\psi_c|$. First, we include spin-independent coherent hopping. Second, the Ising coupling enters the unitary dynamics. Third, we do not include an explicit alignment process. As a consequence, ρ_1 heats up to become completely mixed, $\rho_1(t \rightarrow \infty) \propto \mathbb{1}$, suppressing signatures of quantum active motion in the ensemble-averaged steady state [46].

Importantly, signatures of quantum active motion persist at long times in the pure-state dynamics generated by Eq. (1). We consider measurement-averaged equal-time connected correlation functions,

$$C_{AB}(x) = \overline{\langle \psi_c | A_x B_0 | \psi_c \rangle - \langle \psi_c | A_x | \psi_c \rangle \langle \psi_c | B_0 | \psi_c \rangle}. \quad (4)$$

These exhibit nontrivial behavior due to the second term, which is nonlinear in the system’s density matrix $|\psi_c\rangle\langle\psi_c|$ [30]. Here, A_x and B_0 represent local operators (charge and spin densities as well as currents) at sites x and 0, respectively. We express $C_{AB}(x)$ in terms of the two-replica density matrix averaged over measurement outcomes, $\rho_2 = |\psi_c\rangle\langle\psi_c| \otimes |\psi_c\rangle\langle\psi_c|$. This yields

$$C_{AB}(x) = \frac{1}{2} \left\langle \left(A_x^{(1)} - A_x^{(2)} \right) \left(B_0^{(1)} - B_0^{(2)} \right) \right\rangle, \quad (5)$$

where the superscript indicates action on replica $i = 1, 2$ and $\langle \dots \rangle = \text{tr}(\dots \rho_2)$.

We interpret correlations between the local spin density (“magnetization”) ρ_s and the charge current density j_c as direct signatures of the active propulsion. Below a critical measurement rate, the corresponding steady-state correlations exhibit power-law behavior at long distances, $C_{\rho_s j_c}(x) \sim -\Delta_{sc}/x^2$. We emphasize that these are quantum correlations of a pure-state ensemble and are thus accompanied by significant entanglement. The coefficient Δ_{sc} is an increasing function of γ : activity is driven by the measurements. When γ exceeds a critical strength, the pure-state dynamics undergoes a transition into a phase with exponentially decaying $C_{\rho_s j_c}(x)$. This is summarized in the phase diagram in Fig. 2(a), where g_s is the Luttinger liquid parameter quantifying the Ising interaction (see below). The color scale indicates the active correlations $\propto \Delta_{sc}$, which increase with γ right up to the transition, see Fig. 2(b) for a linecut.

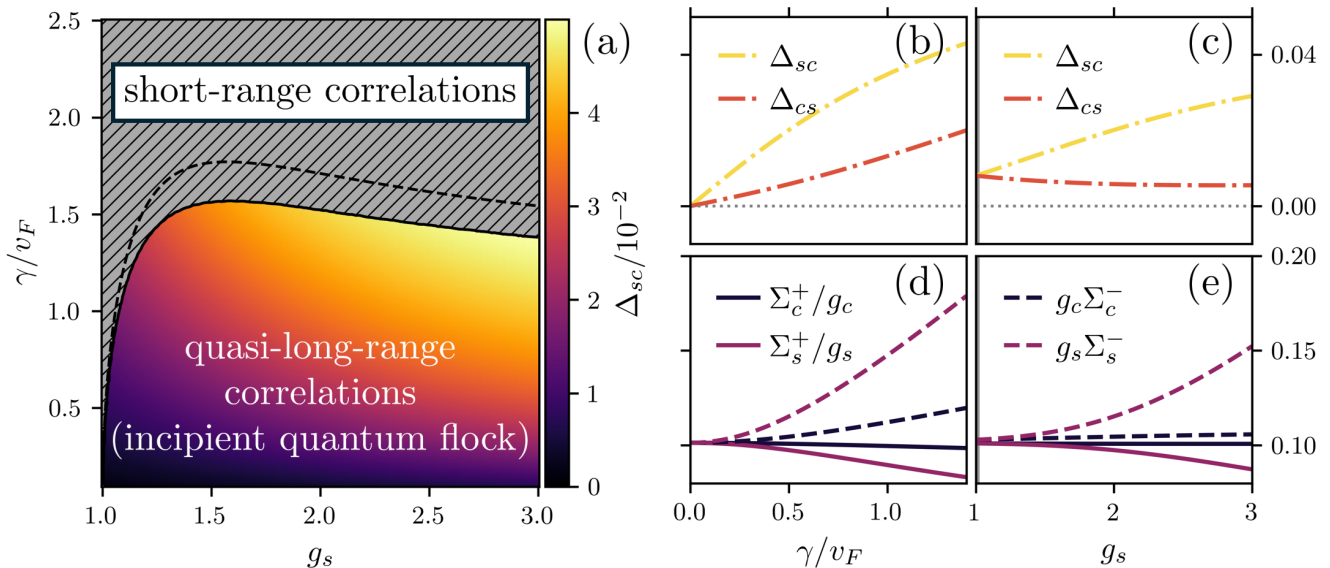


FIG. 2. (a) Phase diagram in the g_s - γ plane obtained from the RG equations (13) with $g_c = 1$ and $\tilde{c} = \tilde{s} = 1/\sqrt{2}$, see Eq. (12). The quasi-long-range quantum active phase (small γ) and the short-range phase (large γ) are separated by a BKT transition (black line). In the quantum active phase, color indicates the magnitude of Δ_{cs} . The dashed line is an analytical estimate for the phase boundary (see main text). (b-e) Dependence of the coefficients $\{\Sigma_{c/s}^\pm, \Delta_{cs/sc}\}$ on γ and g_s , which determine the correlations at the fixed point $\lambda = 0$, see Eq. (15), using $g_s = 2$ in (b) and (d), and $\gamma/v_F = 0.5$ in (c) and (e).

Bosonization.—Rather than working directly with Eqs. (2) and (3), we consider a bosonized continuum model $H \rightarrow H_0 + \delta H$ and $L_{x,\sigma} \rightarrow L_\sigma(x)$ which captures this BKT transition. For generic incommensurate band fillings, the quadratic Hamiltonian

$$H_0 = \frac{v_F}{2} \sum_\nu \int dx \left[(\partial_x \theta_\nu)^2 + \frac{1}{g_\nu^2} (\partial_x \varphi_\nu)^2 \right] \quad (6)$$

describes the dynamics of the charge ($\nu = c$) and spin ($\nu = s$) degrees of freedom in terms of two Luttinger liquids with Fermi velocity v_F . Here, $\partial_x \theta_\nu(x)$ and $\varphi_\nu(x)$ are canonically conjugate real bosonic fields with $[\varphi_\nu(x), \partial_{x'} \theta_{\nu'}(x')] = i\delta_{\nu\nu'} \delta(x-x')$ [24, 47, 48]. Measuring lengths in units of the lattice spacing, the spin sector has the Luttinger parameter $g_s \simeq 1/[1 - J_z/2\pi v_F]^{1/2} > 1$, while $g_c = 1$ in the charge sector. Zeeman and Rashba terms as well as backscattering processes due to J_z give rise to sine-Gordon terms collected in δH (see SM [44]). Similarly, the bosonized measurement operators $L_\sigma(x) = M_\sigma(x) + iK_\sigma(x)$ with hermitian M_σ and K_σ decompose into linear and sine-Gordon terms, $M_\sigma = M_{0,\sigma} + \delta M_\sigma$ and $K_\sigma = K_{0,\sigma} + \delta K_\sigma$. Here,

$$M_{0,\sigma} = \sqrt{\frac{\gamma}{2\pi}} \tilde{c} \partial_x (\varphi_c + \sigma \varphi_s) \sim \text{density}_\sigma, \quad (7a)$$

$$K_{0,\sigma} = \sqrt{\frac{\gamma}{2\pi}} \tilde{s} \sigma \partial_x (\theta_c + \sigma \theta_s) \sim \sigma \times \text{current}_\sigma \quad (7b)$$

stem from momentum-conserving processes. (\tilde{c} and \tilde{s} with $\tilde{c}^2 + \tilde{s}^2 = 1$ are real constants controlled by the

band filling.) The hermitian part $M_{0,\sigma}$ depends on the smooth component $\partial_x (\varphi_c + \sigma \varphi_s)/\sqrt{2}$ of the density of spin- σ particles. Similarly, the antihermitian part $iK_{0,\sigma}$ depends on the smooth component $\sigma \partial_x (\theta_c + \sigma \theta_s)/\sqrt{2}$ of the Hamiltonian current density in σ direction due to spin- σ particles. Further, $2k_F$ processes give rise to the sine-Gordon contributions

$$\delta M_\sigma = \sqrt{\frac{\gamma}{\pi^2}} \sigma \sin \left[2k_F x + \sqrt{2\pi} (\varphi_c + \sigma \varphi_s) \right], \quad (8)$$

while $\delta K_\sigma = 0$. Due to the large difference in momentum transfers, we can treat the $2k_F$ term as a separate measurement process [30]. Thus, there are two sets of jump operators, $L_{0,\sigma} = M_{0,\sigma} + iK_{0,\sigma}$ and $\delta L_\sigma = \delta M_\sigma$. In the bosonized theory, heating of ρ_1 manifests as unbounded growth of the correlation functions $\text{tr}[\chi_{\pm,\nu}(x) \chi_{\pm',\nu'}(x) \rho_1(t)]$ for $t \rightarrow \infty$, where $\chi_{+,\nu} = \varphi_\nu$ and $\chi_{-,\nu} = \theta_\nu$ [29].

Nonhermitian sine-Gordon theory.—We now consider the evolution of the averaged two-replica density matrix ρ_2 . Correlations of charge and spin densities and/or currents can be traced to $C_{AB}(x)$ with $A, B \sim \partial_x \chi_{\pm,\nu}$, which depends only on the relative modes $\chi^{(r)} = (\chi^{(1)} - \chi^{(2)})/\sqrt{2}$, see Eq. (5). Conversely, as a consequence of the heating of ρ_1 , correlations of the center-of-mass (absolute) modes $\chi^{(a)} = (\chi^{(1)} + \chi^{(2)})/\sqrt{2}$ grow without bound for $t \rightarrow \infty$. In fact, symmetry under replica exchange gives $\langle \chi^{(a)} \rangle = \sqrt{2} \text{tr}(\chi \rho_1)$, $\langle \chi^{(r)} \rangle = 0$, and

$$\langle \chi_\alpha^{(a)} \chi_\beta^{(a)} \rangle = 2 \text{tr}(\chi_\alpha \chi_\beta \rho_1) - \langle \chi_\alpha^{(r)} \chi_\beta^{(r)} \rangle. \quad (9)$$

Assuming that correlations of the relative fields remain finite (as confirmed a posteriori), unbounded heating of ρ_1 translates to unbounded heating of correlations in the absolute sector: $\langle \chi_\alpha^{(a)}(x) \chi_\beta^{(a)}(x) \rangle \rightarrow \infty$ and $\langle \chi^{(a)}(x) \rangle = 0$. To arrive at an effective description of the relative sector, we trace out the absolute modes, see SM [44] for details. Importantly, at long times, all contributions from δH become irrelevant under this procedure. Using $\rho_2^{(r)} = \text{tr}^{(a)} \rho_2$, the dynamics in the relative replica sector is then governed by

$$\dot{\rho}_2^{(r)} = -iH_{\text{eff}}^{(r)} \rho_2^{(r)} + i\rho_2^{(r)} [H_{\text{eff}}^{(r)}]^\dagger. \quad (10)$$

Mostly dropping the superscript (r) from now on, the effective nonhermitian sine-Gordon Hamiltonian $H_{\text{eff}} = v_F \int dx (\mathcal{H}_{\text{eff},0} + \delta \mathcal{H}_{\text{eff}})$ is given by

$$\begin{aligned} \mathcal{H}_{\text{eff},0} = & \frac{1}{2} \sum_{\nu=c,s} \left[(\partial_x \theta_\nu)^2 + (k_\nu + \kappa^2) (\partial_x \varphi_\nu)^2 \right] \\ & + \kappa (\partial_x \varphi_c \partial_x \theta_s + c \leftrightarrow s), \end{aligned} \quad (11a)$$

$$\delta \mathcal{H}_{\text{eff}} = i\lambda \cos(\sqrt{4\pi} \varphi_c) \cos(\sqrt{4\pi} \varphi_s), \quad (11b)$$

where we introduced the couplings

$$k_\nu = \frac{1}{g_\nu^2} - \frac{2i\tilde{c}^2\gamma}{\pi v_F} - \kappa^2, \quad \kappa = \frac{\tilde{c}\tilde{s}\gamma}{\pi v_F}, \quad \lambda = \frac{\gamma}{\pi^2 v_F}. \quad (12)$$

Note that γ enters both the parity-odd spin-charge coupling κ (giving rise to $\Delta_{sc} \neq 0$) and the parity-even nonlinearity λ (driving the BKT transition), highlighting the dual role of monitoring for quantum active matter. Importantly, Eq. (10) does not feature a jump term and thus describes the nonhermitian evolution of a pure state, $\rho_2^{(r)} = |\psi\rangle\langle\psi|$, towards a dark state $|\psi(t \rightarrow \infty)\rangle = |0\rangle$. Steady-state connected correlation functions are then given by $C_{AB}(x) = \frac{1}{2} \langle 0 | A^{(r)}(x) B^{(r)}(0) | 0 \rangle$.

Renormalization and phase diagram.—To find $|0\rangle$, we treat the nonlinear term $\propto \lambda$ in Eq. (11) using a perturbative renormalization group (RG) analysis [24, 30]. The one-loop RG equations for the complex couplings (12) are (for a derivation, see SM [44])

$$\frac{d\lambda}{d\ell} = \left(2 - \sum_\nu \frac{1}{\sqrt{k_\nu}} \right) \lambda, \quad \frac{dk_\nu}{d\ell} = -f\lambda^2, \quad (13)$$

where ℓ is the standard RG flow parameter, $|f| \sim \mathcal{O}(1)$ depends weakly on k_ν , and κ is not renormalized. Solving Eq. (13) with the initial values (12) gives the phase diagram in Fig. 2(a). We find a transition between a phase with quasi-long-range quantum active correlations, where $\lambda(\ell \rightarrow \infty) = 0$, and a phase with short-range correlations, where λ flows towards strong coupling. The RG equations (13) are characteristic for a BKT transition [24, 30, 31]. In the quantum active phase, one may assume that k_ν remains unrenormalized since λ quickly approaches zero. The resulting estimate for the phase boundary, $\sum_\nu 1/\sqrt{k_\nu} = 2$, yields the dashed curve in

Fig. 2(a). We find that the quantum active phase disappears without interactions ($g_s \rightarrow 1$).

Gaussian fixed points.—We now study the steady-state correlations $C_{AB}(x)$ for all combinations of $A, B \in \{\varrho_{c/s}, j_{c/s}\}$ at the $|\lambda| \rightarrow 0, \infty$ fixed points. Since these limits correspond to Gaussian fixed points, we obtain exact results for the long-distance behavior. With the mean density ϱ_0 , charge and spin densities are given by $\varrho_\nu = \sqrt{2/\pi} \partial_x \varphi_\nu + \varrho_0 \delta_{\nu,c}$. The respective current densities j_ν include measurement-induced contributions $\propto \kappa$, see Refs. [44, 49–51],

$$j_\nu = -\sqrt{2/\pi} v_F [\partial_x \theta_\nu - \kappa \partial_x \varphi_{\bar{\nu}}] + v_F \kappa \varrho_0 \delta_{\nu,s}, \quad (14)$$

with $\bar{\nu} = s, c$ for $\nu = c, s$. Note that monitoring induces a constant spin-dependent current. Consider first the case $\lambda \rightarrow 0$, where we find

$$\begin{pmatrix} C_{\varrho_\nu \varrho_{\nu'}} & C_{\varrho_\nu j_{\nu'}} \\ C_{j_\nu \varrho_{\nu'}} & C_{j_\nu j_{\nu'}} \end{pmatrix} \simeq -\frac{1}{x^2} \begin{pmatrix} \delta_{\nu\nu'} \Sigma_\nu^+ & v_F \delta_{\nu\bar{\nu}'} \Delta_{\nu\bar{\nu}'} \\ v_F \delta_{\nu\bar{\nu}'} \Delta_{\bar{\nu}\nu} & v_F^2 \delta_{\nu\nu'} \Sigma_\nu^- \end{pmatrix}. \quad (15)$$

The six real coefficients $\{\Sigma_{c/s}^\pm, \Delta_{cs/sc}\}$ are illustrated as functions of γ and/or g_s in Fig. 2(b-e). As in equilibrium Luttinger liquids [24], density-density and current-current correlations decay $\propto x^{-2}$, implying that members of the pure-state ensemble are significantly entangled [30, 52]. Note that spin current (density) correlations are enhanced (reduced) by finite γ and by $g_s > 1$, while charge correlations are not strongly affected. Equation (15) reveals quantum active correlations between spin (charge) densities and charge (spin) currents from the $\Delta_{sc(cs)}$ terms. Notably, Δ_{sc} is enhanced by the Ising interaction while Δ_{cs} is weakened. Finally, consider the strong-coupling phase with large $|\lambda|$. Here, the nonlinearity in Eq. (11) leads to a Gaussian fixed point with a mass term in the boson dispersion (mass m_λ). We then find exponential decay, $C_{A_\nu B_{\nu'}}(x) \propto e^{-|x|/\xi_{\nu\nu'}}$, with the length scale [44]

$$\xi_{\nu\nu'} \sim \frac{v_F}{|m_\lambda|} \max\left(\sqrt{|k_\nu|}, \sqrt{|k_{\nu'}|}\right). \quad (16)$$

We thus encounter only short-range correlations.

Discussion.—We showed that quantum active matter can be realized in monitored interacting fermion chains. Monitoring causes self-propulsion but eventually also drives a BKT transition between phases with algebraic and short-ranged quantum active correlations. The algebraic phase is strongly quantum in that typical pure states cannot be prepared by shallow circuits. The short-range correlated phase is expected to host a second transition to a weakly quantum area-law entangled phase [25–28] with typical pure states preparable by shallow circuits [53]. An explicit study of the entanglement transition is left for future work, as it is currently unknown how to describe it within the bosonization approach [31]. Experimental studies of the quantum active correlations require many copies of the ensemble of measurement trajectories. To deal with the associated

postselection problem [40], one can use methods such as classical-quantum cross-correlations [54], classical postprocessing [55], decoding [56], space-time duality [57], or tree-like measurements [58]. The entanglement transition was successfully observed in this way [59–61]. We expect our work to stimulate theoretical and experimental research on quantum active matter in monitored systems.

ACKNOWLEDGMENTS

We thank Liliana Arrachea, Michael Buchhold, Sebastian Diehl, Rosario Fazio, Igor Gornyi, and Hartmut Löwen for valuable discussions. We acknowledge funding by the Deutsche Forschungsgemeinschaft (DFG, German Research Foundation) under Projektnummer 277101999 - TRR 183 (project B02), under Projektnummer EG 96/14-1, and under Germany's Excellence Strategy - Cluster of Excellence Matter and Light for Quantum Computing (ML4Q) EXC 2004/2 - 390534769. J.F.S. acknowledges the support of the AFOSR MURI program, under Agreement No. FA9550-22-1-0339.

-
- [1] M. C. Marchetti, J. F. Joanny, S. Ramaswamy, T. B. Liverpool, J. Prost, M. Rao, and R. A. Simha, Hydrodynamics of soft active matter, *Rev. Mod. Phys.* **85**, 1143 (2013).
- [2] C. Bechinger, R. Di Leonardo, H. Löwen, C. Reichardt, G. Volpe, and G. Volpe, Active Particles in Complex and Crowded Environments, *Rev. Mod. Phys.* **88**, 045006 (2016).
- [3] S. Ramaswamy, Active matter, *J. Stat. Mech.: Theo. Exp.* **2017**, 054002 (2017).
- [4] S. Shankar, A. Souslov, M. J. Bowick, M. C. Marchetti, and V. Vitelli, Topological active matter, *Nat. Rev. Phys.* **4**, 380 (2022).
- [5] T. Vicsek, A. Czirók, E. Ben-Jacob, I. Cohen, and O. Shochet, Novel type of phase transition in a system of self-driven particles, *Phys. Rev. Lett.* **75**, 1226 (1995).
- [6] A. P. Solon and J. Tailleur, Revisiting the Flocking Transition Using Active Spins, *Phys. Rev. Lett.* **111**, 078101 (2013).
- [7] H. Chaté, Dry Aligning Dilute Active Matter, *Annu. Rev. Condens. Matter Phys.* **11**, 189 (2020).
- [8] B. Benvegnen, H. Chaté, P. L. Krapivsky, J. Tailleur, and A. Solon, Flocking in one dimension: Asters and reversals, *Phys. Rev. E* **106**, 054608 (2022).
- [9] B. VanSaders, M. Fruchart, and V. Vitelli, Measurement-Induced Phase Transitions in Informational Active Matter (2023), [arXiv:2302.07402](https://arxiv.org/abs/2302.07402).
- [10] M. te Vrugt, B. Liebchen, and M. E. Cates, What exactly is 'active matter'? (2025), [arXiv:2507.21621](https://arxiv.org/abs/2507.21621).
- [11] J. Toner and Y. Tu, Long-Range Order in a Two-Dimensional Dynamical XY Model: How Birds Fly Together, *Phys. Rev. Lett.* **75**, 4326 (1995).
- [12] A. P. Solon, H. Chaté, and J. Tailleur, From Phase to Microphase Separation in Flocking Models: The Essential Role of Nonequilibrium Fluctuations, *Phys. Rev. Lett.* **114**, 068101 (2015).
- [13] M. Yamagishi, N. Hatano, and H. Obuse, Proposal of a quantum version of active particles via a nonunitary quantum walk, *Sci. Rep.* **14**, 28648 (2024).
- [14] A. P. Antonov, Y. Zheng, B. Liebchen, and H. Löwen, Engineering active motion in quantum matter, *Phys. Rev. Res.* **7**, 033008 (2025).
- [15] A. P. Antonov, S. Lee, B. Liebchen, H. Löwen, J. Melles, G. Morigi, Y. Tuhkov, and M. te Vrugt, Modeling dissipation in quantum active matter (2025), [arXiv:2511.21502](https://arxiv.org/abs/2511.21502).
- [16] K. Adachi, K. Takasan, and K. Kawaguchi, Activity-induced phase transition in a quantum many-body system, *Phys. Rev. Res.* **4**, 013194 (2022).
- [17] A.-G. Penner, L. Viotti, R. Fazio, L. Arrachea, and F. von Oppen, Heat-to-motion conversion for quantum active matter, *Phys. Rev. B* **112**, L180303 (2025).
- [18] N. Del Ser and V. Lohani, Skyrmion jellyfish in driven chiral magnets, *SciPost Phys.* **15**, 065 (2023).
- [19] D. Hardt, R. Doostani, S. Diehl, N. del Ser, and A. Rosch, Propelling ferrimagnetic domain walls by dynamical frustration, *Nat. Commun.* **16**, 3817 (2025).
- [20] K. Takasan, K. Adachi, and K. Kawaguchi, Activity-induced ferromagnetism in one-dimensional quantum many-body systems, *Phys. Rev. Res.* **6**, 023096 (2024).
- [21] R. Khasseh, S. Wald, R. Moessner, C. A. Weber, and M. Heyl, Active Quantum Flocks, *Phys. Rev. Lett.* **135**, 248302 (2025).
- [22] H. M. Wiseman and G. J. Milburn, *Quantum measurement and control* (Cambridge University Press, 2009).
- [23] R. Fazio, J. Keeling, L. Mazza, and M. Schirò, Many-body open quantum systems, *SciPost Phys. Lect. Notes*, **99** (2025).
- [24] A. O. Gogolin, A. A. Nersisyan, and A. M. Tsvelik, *Bosonization and Strongly Correlated Systems* (Cambridge University Press, 1998).
- [25] F. Barratt, U. Agrawal, S. Gopalakrishnan, D. A. Huse, R. Vasseur, and A. C. Potter, Field Theory of Charge Sharpening in Symmetric Monitored Quantum Circuits, *Physical Review Letters* **129**, 120604 (2022).
- [26] I. Poboiko, P. Pöpperl, I. V. Gornyi, and A. D. Mirlin, Theory of Free Fermions under Random Projective Measurements, *Phys. Rev. X* **13**, 041046 (2023).
- [27] I. Poboiko, P. Pöpperl, I. V. Gornyi, and A. D. Mirlin, Measurement-induced transitions for interacting fermions, *Phys. Rev. B* **111**, 024204 (2025).
- [28] H. Guo, M. S. Foster, C.-M. Jian, and A. W. W. Ludwig, Field theory of monitored interacting fermion dynamics with charge conservation, *Physical Review B* **112**, 064304 (2025).
- [29] M. Buchhold and S. Diehl, Nonequilibrium universality in the heating dynamics of interacting Luttinger liquids,

- Phys. Rev. A* **92**, 013603 (2015).
- [30] M. Buchhold, Y. Minoguchi, A. Altland, and S. Diehl, Effective Theory for the Measurement-Induced Phase Transition of Dirac Fermions, *Phys. Rev. X* **11**, 041004 (2021).
- [31] T. Müller, M. Buchhold, and S. Diehl, Monitored interacting dirac fermions, *Phys. Rev. B* **111**, 174201 (2025).
- [32] B. Skinner, J. Ruhman, and A. Nahum, Measurement-Induced Phase Transitions in the Dynamics of Entanglement, *Phys. Rev. X* **9**, 031009 (2019).
- [33] Y. Li, X. Chen, and M. P. A. Fisher, Quantum Zeno effect and the many-body entanglement transition, *Phys. Rev. B* **98**, 205136 (2018).
- [34] M. J. Gullans and D. A. Huse, Dynamical Purification Phase Transition Induced by Quantum Measurements, *Phys. Rev. X* **10**, 041020 (2020).
- [35] S. Choi, Y. Bao, X.-L. Qi, and E. Altman, Quantum Error Correction in Scrambling Dynamics and Measurement-Induced Phase Transition, *Phys. Rev. Lett.* **125**, 030505 (2020).
- [36] X. Cao, A. Tilloy, and A. De Luca, Entanglement in a fermion chain under continuous monitoring, *SciPost Phys.* **7**, 024 (2019).
- [37] C.-M. Jian, Y.-Z. You, R. Vasseur, and A. W. W. Ludwig, Measurement-induced criticality in random quantum circuits, *Phys. Rev. B* **101**, 104302 (2020).
- [38] Y. Bao, S. Choi, and E. Altman, Theory of the phase transition in random unitary circuits with measurements, *Phys. Rev. B* **101**, 104301 (2020).
- [39] O. Alberton, M. Buchhold, and S. Diehl, Entanglement Transition in a Monitored Free-Fermion Chain: From Extended Criticality to Area Law, *Phys. Rev. Lett.* **126**, 170602 (2021).
- [40] M. P. Fisher, V. Khemani, A. Nahum, and S. Vijay, Random Quantum Circuits, *Annu. Rev. Condens. Matter Phys.* **14**, 335 (2023).
- [41] M. Fava, L. Piroli, T. Swann, D. Bernard, and A. Nahum, Nonlinear Sigma Models for Monitored Dynamics of Free Fermions, *Phys. Rev. X* **13**, 041045 (2023).
- [42] L. Lumia, E. Tirrito, R. Fazio, and M. Collura, Measurement-induced transitions beyond Gaussianity: A single particle description, *Phys. Rev. Res.* **6**, 023176 (2024).
- [43] Y. V. Nazarov and Y. M. Blanter, *Quantum Transport: Introduction to Nanoscience* (Cambridge University Press, Cambridge, UK, 2009).
- [44] See Supplementary Material at [URL] for details of monitoring protocol and the analytical calculations for the bosonized model.
- [45] M. A. Nielsen and I. L. Chuang, *Quantum computation and quantum information* (Cambridge University Press, Cambridge, UK, 2010).
- [46] While the $L_{x,\sigma}$ are not hermitian, one explicitly checks $\mathcal{L}\mathbb{1} = \sum_x (n_{x+\sigma,\sigma} - n_{x,\sigma}) = 0$ with $n_{x,\sigma} = c_{x,\sigma}^\dagger c_{x,\sigma}$ by translation invariance.
- [47] R. Egger and H. Schoeller, RKKY interaction and Kondo screening cloud for strongly correlated electrons, *Phys. Rev. B* **54**, 16337 (1996).
- [48] R. Egger and A. Komnik, Scaling and criticality of the Kondo effect in a Luttinger liquid, *Phys. Rev. B* **57**, 10620 (1998).
- [49] K. V. Hovhannisyanyan and A. Imparato, Quantum current in dissipative systems, *New Journal of Physics* **21**, 052001 (2019).
- [50] P. Pöpperl, I. V. Gornyi, and Y. Gefen, Measurements on an Anderson chain, *Physical Review B* **107**, 174203 (2023).
- [51] L. AntoniĆ, Y. Kafri, D. Podolsky, and A. M. Turner, Motion from measurement: The role of symmetry of quantum measurements, *Physical Review B* **111**, 224305 (2025).
- [52] P. Calabrese and J. Cardy, Entanglement entropy and quantum field theory, *J. Stat. Mech.: Theo. Exp.* **2004**, P06002 (2004).
- [53] R. Suzuki, J. Haferkamp, J. Eisert, and P. Faist, Quantum complexity phase transitions in monitored random circuits, *Quantum* **9**, 1627 (2025).
- [54] S. J. Garratt and E. Altman, Probing Postmeasurement Entanglement without Postselection, *PRX Quantum* **5**, 030311 (2024).
- [55] M. McGinley, Postselection-Free Learning of Measurement-Induced Quantum Dynamics, *PRX Quantum* **5**, 020347 (2024).
- [56] H. Dehghani, A. Lavasani, M. Hafezi, and M. J. Gullans, Neural-network decoders for measurement induced phase transitions, *Nat. Commun.* **14**, 2918 (2023).
- [57] M. Ippoliti and V. Khemani, Postselection-Free Entanglement Dynamics via Spacetime Duality, *Phys. Rev. Lett.* **126**, 060501 (2021).
- [58] X. Feng, J. Côté, S. Kourtis, and B. Skinner, Postselection-free experimental observation of the measurement-induced phase transition in circuits with universal gates, *Commun. Phys.* **10.1038/s42005-025-02443-0** (2026).
- [59] C. Noel, P. Niroula, D. Zhu, A. Risinger, L. Egan, D. Biswas, M. Cetina, A. V. Gorshkov, M. J. Gullans, D. A. Huse, and C. Monroe, Measurement-induced quantum phases realized in a trapped-ion quantum computer, *Nat. Phys.* **18**, 760 (2022).
- [60] J. M. Koh, S.-N. Sun, M. Motta, and A. J. Minnich, Measurement-induced entanglement phase transition on a superconducting quantum processor with mid-circuit readout, *Nat. Phys.* **19**, 1314 (2023).
- [61] J. C. Hoke, M. Ippoliti, E. Rosenberg, D. Abanin, R. Acharya, T. I. Andersen, M. Ansmann, F. Arute, K. Arya, A. Asfaw, and et al. (Google Quantum AI), Measurement-induced entanglement and teleportation on a noisy quantum processor, *Nature* **622**, 481 (2023).
- [62] $\text{diag}(\tilde{h}_{c,q}, \tilde{h}_{s,q})$ contains σ_0 and σ_3 only, so we expect W to contain σ_1 or σ_2 . As argued in the discussion around Eq. (G17), there cannot be a σ_1 contribution.

Appendix A: Directed hopping monitoring protocol

We discuss how monitoring of the jump operators in Eq. (3) can be implemented in a chain of spinful single-level quantum dots with fermion operators $c_{x,\sigma}$. Let us first focus on a spin-polarized system containing, say, only \uparrow -

fermions. To monitor $L_{x,\uparrow}$, sites x and $x+1$ are tunnel-coupled (with strength λ_0) to an auxiliary detector dot each (denoted by 1 and 2 with fermion operators $d_{i \in \{1,2\},\sigma}$), with parameters chosen to facilitate rapid relaxation of the double dot to the detector state $|0_1, \uparrow_2\rangle_d$. The Hamiltonian describing the detector dots including their coupling to sites x and $x+1$ is given by [43]

$$H_{L_{x,\uparrow}} = \lambda_0 \left(d_{1,\uparrow}^\dagger c_{x,\uparrow} + c_{x+1,\uparrow}^\dagger d_{2,\uparrow} + \text{h.c.} \right) + U \left(d_{1,\uparrow}^\dagger d_{1,\uparrow} - \frac{1}{2} \right) \left(d_{2,\uparrow}^\dagger d_{2,\uparrow} - \frac{1}{2} \right) - \delta\mu d_{2,\uparrow}^\dagger d_{2,\uparrow}. \quad (\text{A1})$$

The strongly repulsive Coulomb interaction $U \gg \lambda_0$ enforces empty and doubly-occupied states of the double dot to be high-energy states, and the energy difference $\delta\mu$ with $\lambda_0 < \delta\mu < U/4$ makes $|0_1, \uparrow_2\rangle_d$ the lowest-energy detector state. The double dot thus rapidly relaxes to $|0_1, \uparrow_2\rangle_d$ in the presence of a low-temperature bath.

One now evolves the detector dots coupled to the system for a short time δt , and subsequently projectively measures the charge state of the detector dots. The two possible outcomes are $|0_1, \uparrow_2\rangle_d$ (no cotunneling event; $e = 0$) and $|\uparrow_1, 0_2\rangle_d$ (cotunneling event; $e = 1$). The Kraus operators describing the time evolution of the system state $|\psi\rangle$ follow from [45]

$$\mathcal{K}_e |\psi\rangle = P_e e^{-i\delta t H_{L_{x,\uparrow}}} |\psi\rangle \otimes |0_1, \uparrow_2\rangle_d, \quad (\text{A2})$$

where P_e projects onto outcome e . With the perturbative estimate $\gamma \sim \lambda_0^4 \delta t / U^2$, we find $\mathcal{K}_0 = 1 - \frac{\delta t}{2} L_{x,\uparrow}^\dagger L_{x,\uparrow}$ and $\mathcal{K}_1 = -i\sqrt{\delta t} L_{x,\uparrow}$. Repeating this protocol by exploiting the fast decay of the double dot to reuse Eq. (A2) at each time step, standard arguments give quantum state diffusion, see Eq. (1) with the jump operators $L_{x,\uparrow}$ in Eq. (3) and the measurement rate γ [22]. Next we reintroduce the other spin species. This step does not affect the above process when adding a large Zeeman (or magnetic exchange) field $B \gg \lambda_0$ to the detector dot Hamiltonian, $H_{L_{x,\uparrow}} \rightarrow H_{L_{x,\uparrow}} + B \sum_i d_{i,\downarrow}^\dagger d_{i,\downarrow}$, effectively forbidding \downarrow -electrons to enter the double dot. The required hierarchy of timescales is summarized as follows. The decay time of the double dot and the time to projectively measure the double dot charge state should be much smaller than U^{-1} , while at the same time we assume $U^{-1} \ll \delta t, \lambda_0^{-1}$. Finally, the relevant system time scales should be large against δt and λ_0^{-1} . The construction of $L_{x,\downarrow}$ proceeds analogously.

Appendix B: Bosonization conventions

For convenience, we briefly summarize our bosonization conventions following Ref. [48]. First, we let $c_{x,\sigma} \rightarrow \sqrt{a}\psi_\sigma(x)$. We set the lattice constant $a \equiv 1$, i.e., we measure lengths in units of a . The fermionic field $\psi_\sigma(x)$ is decomposed into left and right moving contributions near the Fermi points $\pm k_F$, $\psi_\sigma(x) \rightarrow \sum_{p=\pm} \psi_{\sigma,p}(x)$. We bosonize the latter fields via

$$\psi_{\sigma,p}(x) = \frac{\eta_{\sigma,p}}{\sqrt{2\pi}} e^{ipk_F x - i\sqrt{\pi}\theta_\sigma(x) + ip\sqrt{\pi}\varphi_\sigma(x)}, \quad (\text{B1})$$

where $\theta_\sigma = (\theta_c + \sigma\theta_s)/\sqrt{2}$ and $\varphi_\sigma = (\varphi_c + \sigma\varphi_s)/\sqrt{2}$. Anticommutation is enforced by Klein factors which can be written as Majorana operators $\eta_{\sigma,p}$ satisfying $\eta_{\sigma,p}^2 = 1$. As we restrict attention to correlations of fermion bilinears (densities and/or currents), we may parameterize their products by Pauli matrices $\beta_{1,2,3}$ acting on an auxiliary Hilbert space,

$$\eta_{\sigma,p}\eta_{\sigma,-p} = ip\sigma\beta_3, \quad \eta_{\sigma,p}\eta_{-\sigma,p} = i\sigma\beta_2, \quad \eta_{\sigma,p}\eta_{-\sigma,-p} = ip\beta_1. \quad (\text{B2})$$

Applying these bosonization rules, we obtain the bosonized Hamiltonian in Eq. (6) and the linear piece of the bosonized jump operators in Eq. (7). Note that we dropped a constant contribution to $M_{0,\sigma}$ proportional to the overall charge density ϱ_0 . Keeping this term gives rise to a contribution $\propto \int dx \partial_x \theta_s$ to the Hamiltonian which does not affect the dynamics. One furthermore finds the nonlinear piece in Eq. (8), which should technically be multiplied by β_3 . In the absence of spin-flip terms, one can simply fix $\beta_3 = 1$ since no other β_i feature in the problem. Spin-flip terms lead to contributions $\propto \beta_2$, such that one in principle needs to keep the auxiliary Pauli structure. However, the steady state is independent of such terms as, upon tracing over the absolute replica sector, no dependence on spin-flip processes remains. This is explained in detail below.

Appendix C: Replica master equation

Consider a monitored system evolving under the stochastic Schrödinger equation (1). The ensemble-averaged two-replica state $\rho_2(t)$ then evolves according to

$$\dot{\rho}_2 = \left(\mathcal{L}^{(1)} + \mathcal{L}^{(2)} \right) \rho_2 + \sum_{\mu} \overline{\mathcal{R}[\tilde{L}_{\mu}] \rho_c \otimes \mathcal{R}[\tilde{L}_{\mu}] \rho_c}. \quad (\text{C1})$$

Here, $\rho_c = |\psi_c\rangle\langle\psi_c|$ and we define the single-replica Liouvillian as $\mathcal{L}\rho = -i[H, \rho] + \sum_{\mu} \mathcal{D}[L_{\mu}]\rho$. We also introduced the multi-index $\mu = (x, \sigma)$ and the shorthands $\mathcal{D}[L]\rho = L\rho L^{\dagger} - \frac{1}{2}\{L^{\dagger}L, \rho\}$ with the anticommutator $\{\cdot, \cdot\}$, $\mathcal{R}[L]\rho = L\rho + (L\rho)^{\dagger}$, and $\tilde{L}\rho = L\rho - \text{tr}(L\rho)\rho$. Consider the last term in Eq. (C1). It contains third- and fourth-order terms in the system state, which couple the problem to sectors with higher replica number. With $M = (L + L^{\dagger})/2$, we proceed by the approximate decoupling

$$\overline{\mathcal{R}[L]\rho_c \otimes \rho_c} \simeq 2 \langle M^{(i)} \rangle \rho_2, \quad \overline{\text{tr}^2(\mathcal{R}[L]\rho_c \otimes \rho_c)} \simeq 4 \langle M^{(1)} M^{(2)} \rangle \rho_2. \quad (\text{C2})$$

We emphasize that this decoupling step yields identical results as calculations based on a linear stochastic master equation employing the standard replica trick to connect to physical observables [31, 41]. Expectation values that only depend on a single replica are simply those of the measurement-averaged state, $\langle M^{(i)} \rangle = \text{tr}(M\rho_c) \text{tr}(\rho_c) = \text{tr}(M\rho_1)$. These expectation values vanish at sufficiently late times due to the heating-up of ρ_1 and the tracelessness of M . Enforcing conservation of $\text{tr}(\rho_2)$, we obtain

$$\dot{\rho}_2 = \sum_i \mathcal{L}^{(i)} \rho_2 + \sum_{\mu} \mathcal{R}[L_{\mu}^{(1)}] \mathcal{R}[L_{\mu}^{(2)}] \rho_2 - \mathcal{N} \rho_2, \quad (\text{C3})$$

where $\mathcal{N} = 4 \sum_{\mu} \langle M_{\mu}^{(1)} M_{\mu}^{(2)} \rangle$.

In the bosonized continuum framework, after introducing relative (r) and absolute (a) boson fields in replica space, Eq. (C3) takes the form

$$\dot{\rho}_2 = \left(\mathcal{L}_0^{(a)} + \mathcal{L}_0^{(r)} + \delta\mathcal{L} \right) \rho_2. \quad (\text{C4})$$

Here, $\mathcal{L}_0^{(a)}$ and $\mathcal{L}_0^{(r)}$ originate from terms that are at most quadratic in the fields, i.e., those involving H_0 and $L_{0,\sigma}$. They contain only (a) or (r) fields, respectively. Specifically, they are given by

$$\mathcal{L}_0^{(a)} \rho_2 = \mathcal{R}[-iH_{\text{eff},0}^{(a)}] \rho_2 + 2 \sum_{\mu} \mathcal{D}[L_{0,\mu}^{(a)}] \rho_2, \quad \mathcal{L}_0^{(r)} \rho_2 = \mathcal{R}[-iH_{\text{eff},0}^{(r)}] \rho_2. \quad (\text{C5})$$

With $H_0^{(\zeta)}$ obtained from Eq. (6), the effective Hamiltonians for absolute and relative sectors ($\zeta \in \{a, r\}$) have opposite signs for the measurement-induced terms,

$$H_{\text{eff},0}^{(\zeta)} = H_0^{(\zeta)} \mp_{\zeta} \sum_{\mu} \left\{ M_{0,\mu}^{(\zeta)} K_{0,\mu}^{(\zeta)} - i \left[(M_{0,\mu}^{(\zeta)})^2 - \langle (M_{0,\mu}^{(\zeta)})^2 \rangle \right] \right\}, \quad (\text{C6})$$

with $\mp_a = -$ and $\mp_r = +$. The operators $M_{0,\mu}^{(\zeta)}$ and $K_{0,\mu}^{(\zeta)}$ similarly follow from Eqs. (7) by using relative or absolute boson fields. Nonlinear contributions originate from δH and δL_{σ} . In Eq. (C4), these terms are collected in the Lindbladian term ($i, j = 1, 2$)

$$\delta\mathcal{L} \rho_2 = -i \sum_i [\delta H^{(i)}, \rho_2] + \sum_{ij,\mu} \left(\delta M_{\mu}^{(i)} \rho_2 \delta M_{\mu}^{(j)} - \frac{(-1)^{i+j}}{2} \{ \delta M_{\mu}^{(i)} \delta M_{\mu}^{(j)}, \rho_2 \} - \langle \delta M_{\mu}^{(1)} \delta M_{\mu}^{(2)} \rangle \rho_2 \right), \quad (\text{C7})$$

where $\delta H = \delta H_{\text{Ising}} + H_{\text{flip}}$ combines backscattering effects due to the Ising interaction and spin-flip terms, and $\delta M_{\mu}^{(i)}$ is given by Eq. (8). For clarity, let us now focus on the Zeeman coupling, but using the Rashba term—or both terms together—instead of the Zeeman coupling yields identical conclusions at long times after averaging over the absolute replica sector. In bosonized language, with the Pauli matrix β_2 in Eq. (B2), we find the Hamiltonian contributions

$$\delta H_{\text{Ising}} \sim -\beta_2 \int dx \cos(\sqrt{8\pi}\varphi_s), \quad H_{\text{flip}} \sim -\beta_2 \int dx \sin(\sqrt{2\pi}\theta_s) \cos(\sqrt{2\pi}\varphi_s). \quad (\text{C8})$$

At long times, both terms do not contribute to ρ_2 after averaging over the absolute mode.

Appendix D: Average over the absolute mode

Taking into account that the absolute replica sector heats up for $t \rightarrow \infty$ and that $C_{AB}(x)$ involves only fields in the relative sector, we next perform a trace over the absolute modes on both sides of Eq. (C4). We thereby arrive at an effective equation of motion for the density operator $\rho_2^{(r)} = \text{tr}^{(a)}(\rho_2)$ describing the relative sector. At long times, the factorization $\rho_2 \simeq \rho_2^{(a)} \otimes \rho_2^{(r)}$ applies, where $\rho_2^{(a)}$ describes the diverging bosonic fluctuations in the absolute sector. Let us begin by considering contributions due to $\delta\mathcal{L}$ in Eq. (C7). We then note that $\text{tr}^{(a)}(\delta H^{(i)} \rho_2^{(a)}) \rightarrow 0$ while one has

$$\text{tr}^{(a)} \left[\left\{ \left(\delta M_\sigma^{(1)} - \delta M_\sigma^{(2)} \right)^2, \rho_2^{(a)} \otimes \rho_2^{(r)} \right\} \right] = \frac{\gamma}{\pi^2} \left\{ 1 - \cos \left(\sqrt{8\pi} \varphi_\sigma^{(r)} \right), \rho_2^{(r)} \right\}, \quad (\text{D1})$$

where $\varphi_\sigma = (\varphi_c + \sigma \varphi_s) / \sqrt{2}$. Using the above product ansatz for ρ_2 in a naive manner, the term $\text{tr}^{(a)}[\sum_{ij} \delta M_\mu^{(i)} \rho_2 \delta M_\mu^{(j)}]$ in Eq. (C7) appears to give a finite contribution. However, a more careful analysis based on the corresponding Keldysh action [30, 31] shows that this term vanishes upon tracing over the absolute modes. In fact, it depends on inter-contour correlation functions of the type $\exp\{-2\pi \langle (\varphi_+^{(a)} \pm \varphi_-^{(a)})^2 \rangle\}$, where \pm labels the Keldysh forward and backward contours. While usually correlations of the quantum component $\langle (\varphi_+^{(a)} - \varphi_-^{(a)})^2 \rangle$ are guaranteed to vanish by causality [43], this does not hold true for the replicated monitored theory, where $\langle (\varphi_+^{(a)} \pm \varphi_-^{(a)})^2 \rangle$ grows unboundedly for both signs. We therefore drop the corresponding exponentiated terms as well as the associated contributions to the normalization term. Altogether, after summing over σ , we find

$$\text{tr}^{(a)}(\delta\mathcal{L} \rho_2) \simeq \frac{\gamma}{\pi^2} \int dx \left[\left\{ \cos \left(\sqrt{4\pi} \varphi_c^{(r)} \right) \cos \left(\sqrt{4\pi} \varphi_s^{(r)} \right), \rho_2^{(r)} \right\} - 2 \left\langle \cos \left(\sqrt{4\pi} \varphi_c^{(r)} \right) \cos \left(\sqrt{4\pi} \varphi_s^{(r)} \right) \right\rangle \rho_2^{(r)} \right]. \quad (\text{D2})$$

Dropping normalization terms for ease of presentation, and collecting the different contributions to

$$\dot{\rho}_2^{(r)} = \text{tr}^{(a)}(\dot{\rho}_2) = \mathcal{L}_0^{(r)} \rho_2^{(r)} + \text{tr}^{(a)}(\delta\mathcal{L} \rho_2), \quad (\text{D3})$$

we obtain Eqs. (10) and (11).

Appendix E: Derivation of the RG flow equations

We evaluate the long-distance behavior of correlation functions in the presence of the nonlinear sine-Gordon terms in the nonhermitian effective Hamiltonian. To this end, we introduce a field theory which enables a perturbative one-loop RG calculation. Mostly dropping the (r) label indicating the relative replica sector, in order to define the field theory, consider the solution to Eq. (10), $\rho^{(r)}(t) = \frac{|\psi(t)\rangle\langle\psi(t)|}{\langle\psi(t)|\psi(t)\rangle}$, where we explicitly normalize and use $|\psi(t)\rangle = e^{-iH_{\text{eff}}t} |\psi(0)\rangle$ with the nonhermitian sine-Gordon Hamiltonian H_{eff} in Eq. (11). The initial state $|\psi(0)\rangle$ is not important since the evolution drives any initial state to the same dark state for $t \rightarrow \infty$. Using standard techniques, we write the time evolution operator (at long times) as functional integral, $e^{-iH_{\text{eff}}t} \rightarrow \int \mathcal{D}\varphi e^{iS[\varphi]}$, with the real-time action $S[\varphi] = S_0[\varphi] + S_\kappa[\varphi] + S_\lambda[\varphi]$. Here, we have separated the action into Gaussian ($S_0 + S_\kappa$) and nonlinear parts (S_λ). Rescaling $t \rightarrow t/v_F$, with the couplings in Eq. (12), we find

$$\begin{aligned} S_0 &= \frac{1}{2} \int_{t,x} \sum_{\nu=c,s} [l_\nu (\partial_t \varphi_\nu)^2 - k_\nu (\partial_x \varphi_\nu)^2], & S_\kappa &= -\kappa \int_{t,x} [\partial_x \varphi_c \partial_t \varphi_s + (c \leftrightarrow s)], \\ S_\lambda &= -i\lambda \int_{t,x} \cos(\sqrt{4\pi} \varphi_c) \cos(\sqrt{4\pi} \varphi_s). \end{aligned} \quad (\text{E1})$$

We note that the κ^2 term in $\mathcal{H}_{\text{eff},0}$, see Eq. (11), cancels out when switching to the corresponding action S_0 . To capture renormalization effects of the Fermi velocity v_F , we also introduced the couplings l_ν in S_0 , with $l_\nu = 1$ in the ultraviolet. We proceed by performing a standard one-loop momentum-shell renormalization [24], employing a space-time symmetric frequency and momentum cutoff Λ . With the flow parameter ℓ such that $d\ell = -d \ln \Lambda$, we find the RG equations

$$\frac{d\lambda}{d\ell} = \left(2 - \sum_\nu \frac{1}{\sqrt{l_\nu k_\nu}} \right) \lambda, \quad \frac{dl_\nu}{d\ell} = f_t \lambda^2, \quad \frac{dk_\nu}{d\ell} = -f_x \lambda^2. \quad (\text{E2})$$

We here assumed $\text{Im}(l_\nu k_\nu) < 0$ to hold during the entire RG flow, which has been confirmed numerically throughout the perturbative RG regime with $|\lambda(\ell)| \lesssim 1$. With $l_\nu(0) = 1$, we find $l_c(\ell) = l_s(\ell) = l(\ell)$ for all ℓ . In Eq. (E2), we also introduced the real numbers f_t and f_x through the relation

$$\begin{pmatrix} f_t \\ f_x \end{pmatrix} = -\frac{1}{2\Lambda^4} \int_0^{1/\Lambda} dR R^3 \int_0^{2\pi} d\chi \begin{pmatrix} \cos^2 \chi \\ \sin^2 \chi \end{pmatrix} \int_0^{2\pi} d\vartheta \sum_{\nu=c,s} \frac{e^{-iR \cos(\chi+\vartheta)}}{l_\nu \cos^2 \vartheta - k_\nu \sin^2 \vartheta}. \quad (\text{E3})$$

For $\Lambda \sim 1$, we find $f_t \simeq f_x$ and thus set $f_t = f_x = f$ in Eq. (13), with $|f| \sim \mathcal{O}(1)$. Further, in the perturbative regime, $l(\ell)$ does not significantly depart from its initial value $l(0) = 1$, and we therefore drop this factor in Eq. (13). For the results shown in Fig. 2(a) of the main text, we have numerically integrated the full RG equations (E2), with $f_{t,x}$ in Eq. (E3) and setting $\Lambda = 1$. To determine the phase boundary, we integrate Eq. (E2) from $\ell = 0$ to $\ell_{\text{max}} = 50$, using as initial data $\lambda(0) = \lambda$, $l_\nu(0) = 1$, and $k_\nu(0) = k_\nu$, see Eq. (12). The strong vs weak coupling phases are identified through the criterion $|\lambda(\ell_{\text{max}})/\lambda(0)| \gtrsim 1$.

Appendix F: Current operator

In addition to the usual Hamiltonian contribution, the current operator can also receive contributions originating from quantum jumps described by $L_{j,\sigma}$ in Eq. (3), see Ref. [51]. To identify the corresponding bosonized current operator, we consider the (measurement-averaged) Heisenberg picture evolution of $Q_\sigma(x) = \int_{-\infty}^x dx' \varrho_\sigma(x')$, where $\varrho_\sigma(x) = \frac{1}{\sqrt{\pi}} \partial_x \varphi_\sigma(x) + (2k_F\text{-terms})$ is the local density variation of spin- σ fermions. By charge conservation, we identify the local current as $j_\sigma(x) = -\dot{Q}_\sigma(x)$. (In this expression, we have assumed that spin-flip processes are irrelevant, as is the case after averaging over the absolute replica sector. In the presence of spin-flip processes, only the charge current $\sum_\sigma j_\sigma(x)$ is well-defined.) The full spin-resolved current density, including measurement-induced current operators, may then be evaluated by using the Lindblad equation, resulting in

$$\dot{Q}_\sigma(x) = \mathcal{L}^\dagger Q_\sigma(x), \quad \mathcal{L}^\dagger \mathcal{O} = i[H, \mathcal{O}] + \sum_\mu (L_\mu^\dagger \mathcal{O} L_\mu - \frac{1}{2} \{L_\mu^\dagger L_\mu, \mathcal{O}\}). \quad (\text{F1})$$

Dropping rapidly oscillating contributions, i.e., setting $\varrho_\sigma(x) \equiv \frac{1}{\sqrt{\pi}} \dot{\varphi}_\sigma(x)$ [24], we arrive at

$$j_\sigma(x) = -\frac{v_F}{\sqrt{\pi}} \partial_x \theta_\sigma(x) + \frac{v_F \kappa}{\sqrt{\pi}} \sigma \partial_x \varphi_\sigma(x) + \sigma \frac{j_0}{2}, \quad (\text{F2})$$

where $j_0 = v_F \kappa \varrho_0$ depends on the average fermion density ϱ_0 in the system. The first term in Eq. (F2) comes from the Hamiltonian contribution, while the two other terms are due to measurement-induced currents. In fact, with κ in Eq. (12), the spin-dependent average current $\sigma j_0/2$ in Eq. (F2) depends linearly on the monitoring strength γ and highlights the quantum active motion of particles exposed to this monitoring protocol. Forming charge and spin current densities via $j_c = \sum_\sigma j_\sigma$ and $j_s = \sum_\sigma \sigma j_\sigma$, we obtain Eq. (14). Notably, current operators of similar form can be obtained by gauging the $U(1)$ charge and spin symmetries of the effective Hamiltonians in Eq. (C6). With our conventions and $\zeta \in \{a, r\}$, minimal coupling is implemented through the replacement $\partial_x \theta_\nu^{(\zeta)}(x) \rightarrow \partial_x \theta_\nu^{(\zeta)}(x) + \sqrt{\frac{2}{\pi}} \mathcal{A}_\nu(x)$. This gives the minimal coupling currents

$$j_{\text{mc};\nu}^{(\zeta)}(x) = -\frac{\delta H_{\text{eff},0}^{(\zeta)}}{\delta \mathcal{A}_\nu(x)} = -\frac{v_F}{\sqrt{\pi}/2} \left[\partial_x \theta_\nu^{(\zeta)} \mp_\zeta \kappa \partial_x \varphi_\nu^{(\zeta)} \right], \quad (\text{F3})$$

where again $\mp_a = -$ and $\mp_r = +$. Note the difference in relative sign to Eq. (14) for $\zeta = r$. This has important implications for the RG flow of connected correlation functions involving $j_\nu^{(r)}$: Only the relative replica sector $U(1)$ charge densities and the associated minimal coupling currents remain normalized under the RG flow, i.e., $\varrho_\nu^{(r)}(x)|_{\text{UV}} = \varrho_\nu^{(r)}|_{\text{IR}} + \dots$ and $j_{\text{mc};\nu}^{(r)}(x)|_{\text{UV}} = j_{\text{mc};\nu}^{(r)}(x)|_{\text{IR}} + \dots$, where ellipses refer to irrelevant operators. However, we are interested in the connected correlations of the current operator defined in Eq. (14). Using Eqs. (4) and (5), this translates to correlations involving $j_\nu^{(r)} = j_{\text{mc};\nu}^{(r)} + 2v_F \kappa \varrho_\nu^{(r)}$. Under the RG flow, this maps to $j_\nu^{(r)}|_{\text{UV}} = j_{\text{mc};\nu}^{(r)}|_{\text{IR}} + 2v_F \kappa \varrho_\nu^{(r)}|_{\text{IR}} + \dots$, and by denoting the parameters of the renormalized action as v'_F and κ' , we thus find

$$j_\nu^{(r)}|_{\text{UV}} = -\sqrt{\frac{2}{\pi}} [v'_F \partial_x \theta_c + (2v_F \kappa - v'_F \kappa') \partial_x \varphi_s]|_{\text{IR}} + \dots \quad (\text{F4})$$

Since neither v_F , as captured by the RG flow of $l(\ell)$, nor κ are significantly renormalized during the perturbative RG flow, we set $2v_F\kappa - v_F'\kappa' \simeq v_F\kappa$. In the main text, we thereby neglect the weak renormalization of measurement-induced currents.

Appendix G: Correlations at the Gaussian fixed points

We compute the steady-state correlation functions $C_{AB}(x)$ at the fixed points describing either the weak-coupling limit (with $\lambda \rightarrow 0$) or the strong-coupling limit (with $|\lambda| \rightarrow \infty$). Both fixed points are described by a Gaussian theory H_{gfp} in terms of boson mode operators, see also Ref. [30]. This fact allows us to obtain exact results for $C_{AB}(x)$. Suppressing the (r) superscript again, we expand the bosonic fields $\varphi_\nu(x)$ and $\theta_\nu(x)$ by using bosonic mode operators $b_{\nu,q}$ with the algebra $[b_{\nu,q}, b_{\nu',q'}^\dagger] = \delta_{\nu\nu'}\delta_{qq'}$ [24]. Specifically, we have

$$\varphi_\nu(x) = \sum_q \sqrt{\frac{v_F}{2L|\omega_{\nu,q}|}} e^{iqx} (b_{\nu,q}^\dagger + b_{\nu,-q}), \quad \partial_x \theta_\nu(x) = i \sum_q \sqrt{\frac{|\omega_{\nu,q}|}{2Lv_F}} e^{iqx} (b_{\nu,q}^\dagger - b_{\nu,-q}), \quad (\text{G1})$$

with the complex dispersion relation

$$\omega_{\nu,q}^2 = \tilde{k}_\nu v_F^2 q^2 - im_\lambda^2, \quad \tilde{k}_\nu \equiv k_\nu + \kappa^2. \quad (\text{G2})$$

Here, we have $m_\lambda = 0$ at the weak-coupling fixed point, while the nonhermitian sine-Gordon term yields a finite value for the ‘‘mass’’ m_λ at strong coupling. We note that for $\gamma > 0$, we have $\text{Im}(\omega_{\nu,q}) < 0$, see Eq. (12). With bosonic spinor operators B_q , the fixed-point Hamiltonian has the Gaussian form

$$H_{\text{gfp}} = \frac{1}{2} \sum_q B_q^\dagger h_q B_q, \quad B_q = \begin{pmatrix} b_{c,q}, b_{s,q}, b_{c,-q}, b_{s,-q} \end{pmatrix}^\top, \quad h_q = \begin{pmatrix} h_{c,q} & 0 \\ 0 & h_{s,q} \end{pmatrix}_\sigma + v_F q (\kappa_{q,+} \sigma_1 \tau_3 - \kappa_{q,-} \sigma_2 \tau_2), \quad (\text{G3})$$

where the Hamiltonian matrix h_q and the operators B_q are defined in a combined charge-spin and Nambu (particle-hole) space. In particular, the $h_{\nu,q}$ in Eq. (G3) correspond to the Nambu matrices

$$h_{\nu,q} = \frac{|\omega_{\nu,q}|}{2} [(e^{i\eta_{\nu,q}} + 1)\tau_0 + (e^{i\eta_{\nu,q}} - 1)\tau_1], \quad \eta_{\nu,q} = 2 \arg(\omega_{\nu,q}). \quad (\text{G4})$$

Here and below, the subscripts σ and τ refer to charge-spin ($\nu, \nu' = c, s$) and Nambu space, respectively. Similarly, Pauli matrices σ_i (τ_i) act in charge-spin (Nambu) space. In Eq. (G3), we also used the couplings

$$\kappa_{q,\pm} = \frac{\kappa}{2} \left(\sqrt{\left| \frac{\omega_{c,q}}{\omega_{s,q}} \right|} \pm \sqrt{\left| \frac{\omega_{s,q}}{\omega_{c,q}} \right|} \right). \quad (\text{G5})$$

To identify the dark state $|0\rangle$, we perform a Bogoliubov transformation, $B_q = V_q \tilde{B}_q$, in order to bring $\tilde{h}_q = V_q^\dagger h_q V_q$ into lower triangular form in Nambu space. Note that V_q is not unitary but rather satisfies $V_q^\dagger \tau_3 V_q = \tau_3$. With indices referring to the Nambu basis, the Hamiltonian is then given by

$$H_{\text{gfp}} = \sum_q \left(\tilde{b}_q^\dagger \tilde{h}_{q,11} \tilde{b}_q + \frac{1}{2} \tilde{b}_{-q} \tilde{h}_{q,21} \tilde{b}_q \right). \quad (\text{G6})$$

The dark state is identified as the unique state annihilated by the \tilde{b}_q bosons, $\tilde{b}_q |0\rangle = 0$.

Steady-state equal-time correlation functions $C_{AB}(x)$ are simply correlations in the state $|0\rangle$. We are interested in correlation functions of charge and spin currents, j_ν , and of the respective densities, $\rho_{\nu'}$. Using Eq. (14) for j_ν (and similarly for ρ_ν , see main text), these correlation functions can be decomposed as

$$C_{\rho_\nu \rho_{\nu'}}(x) = \frac{2}{\pi} F_{\nu\nu'}^{++}(x), \quad C_{j_\nu j_{\nu'}}(x) = -\frac{2}{\pi} v_F [F_{\nu\nu'}^{+-}(x) - \kappa F_{\nu\nu'}^{++}(x)], \quad (\text{G7})$$

$$C_{j_\nu \rho_{\nu'}}(x) = -\frac{2}{\pi} v_F [F_{\nu\nu'}^{-+}(x) - \kappa F_{\nu\nu'}^{++}(x)], \quad C_{j_\nu j_{\nu'}}(x) = \frac{2}{\pi} v_F^2 [F_{\nu\nu'}^{--}(x) + \kappa^2 F_{\nu\nu'}^{++}(x) - \kappa (F_{\nu\nu'}^{-+}(x) + F_{\nu\nu'}^{+-}(x))],$$

with the correlation functions ($\alpha, \alpha' = \pm$)

$$F_{\nu\nu'}^{\alpha\alpha'}(x) = \langle 0 | \partial_x \chi_{\alpha,\nu}(x) \partial_x \chi_{\alpha',\nu'}(0) | 0 \rangle. \quad (\text{G8})$$

We recall that $\chi_{+,\nu} = \varphi_\nu$ and $\chi_{-,\nu} = \theta_\nu$. In Eqs. (G7), terms proportional to κ or κ^2 originate from measurement-induced currents. We note that the constant measurement-induced spin current $j_0 = v_F \kappa \rho_0$ does not affect connected correlation functions. Taking the $L \rightarrow \infty$ limit, Eq. (G8) can be written as

$$F_{\nu\nu'}^{\alpha\alpha'}(x) = \int \frac{dq}{8\pi} e^{iqx} q \left(\frac{v_F q}{|\omega_{\nu,q}|} \right)^{\frac{\alpha}{2}} \left(\frac{v_F q}{|\omega_{\nu',q}|} \right)^{\frac{\alpha'}{2}} \left[\text{tr} \left(V_q^\dagger M_{\nu\nu'}^{\alpha\alpha'} V_q \right) - 2\delta_{\nu\nu'}(1 - \delta_{\alpha\alpha'}) \right], \quad M_{\nu\nu'}^{\alpha\alpha'} = |\nu\rangle\langle\nu'|_\sigma \otimes \begin{pmatrix} 1 & \alpha' \\ \alpha & \alpha\alpha' \end{pmatrix}. \quad (\text{G9})$$

We can argue on general grounds that there are no correlations between the charge fields χ_c and the spin fields χ_s if $g_c = g_s$. In this case, $h_{c,q} = h_{s,q} \equiv h_{0,q}$ and $\kappa_{q,-} = 0$, such that one can write the single-particle Hamiltonian as $h_q = \sigma_0 h_{0,q} + \kappa q \sigma_1 \tau_3$. Note that $\sigma_1 = \pm 1$ corresponds to spins \uparrow and \downarrow , respectively, i.e., the system decouples into two independent non-hermitian Luttinger liquids. In particular, due to the absence of spin-structure in the first term, one can choose $V_q \propto \sigma_0$. Further, due to $V_q^\dagger \tau_3 V_q = \tau_3$, the κ -term does not affect the transformation V_q . As a consequence, the correlation functions F are independent of κ and vanish for cross-correlations between the spin- σ sectors, and also for cross-correlations between the spin and charge sector. However, correlations between the spin/charge density and the charge/spin current persist even for $g_c = g_s$ due to the κ -term in Eq. (14).

1. Weak-coupling fixed point

We now proceed by evaluating the correlation functions F . Consider first the massless case, $m_\lambda = 0$, corresponding to the fixed point of the quasi-long-range quantum active phase. Here, we have $|\omega_{\nu,q}| = |\sqrt{k_\nu} v_F q|$, and the only nontrivial momentum dependence of h_q stems from the sign of q in the κ term in Eq. (G3). Thus, the transformation V_q depends only on the sign of q , allowing us to decompose

$$\text{tr} \left(V_q^\dagger M_{\nu\nu'}^{\alpha\alpha'} V_q - M_{\nu\nu'}^{\alpha\alpha'} \tau_3 \right) = \tilde{\Sigma}_{\nu\nu'}^{\alpha\alpha'} + \text{sgn}(q) \tilde{\Delta}_{\nu\nu'}^{\alpha\alpha'}, \quad (\text{G10})$$

in terms of the momentum-independent coefficients

$$\tilde{\Sigma}_{\nu\nu'}^{\alpha\alpha'} = \frac{1}{2} \sum_{\pm} \text{tr} \left(V_{\pm}^\dagger M_{\nu\nu'}^{\alpha\alpha'} V_{\pm} \right) - \delta_{\nu\nu'}(1 - \delta_{\alpha\alpha'}), \quad \tilde{\Delta}_{\nu\nu'}^{\alpha\alpha'} = \frac{1}{2} \sum_{\pm} (\pm) \text{tr} \left(V_{\pm}^\dagger M_{\nu\nu'}^{\alpha\alpha'} V_{\pm} \right). \quad (\text{G11})$$

Here, we defined $V_+ = V_{q>0}$ and $V_- = V_{q<0}$. They are not independent: The relation $V_- = \tau_1 V_+^* \tau_1$ implies

$$\text{tr} \left(V_-^\dagger M_{\nu\nu'}^{\alpha\alpha'} V_- \right) = \alpha\alpha' \text{tr} \left(V_+^\dagger M_{\nu\nu'}^{\alpha\alpha'} V_+ \right). \quad (\text{G12})$$

Equation (G9) then becomes

$$F_{\nu\nu'}^{\alpha\alpha'}(x) = |\tilde{k}_\nu|^{-\frac{\alpha}{4}} |\tilde{k}_{\nu'}|^{-\frac{\alpha'}{4}} \int \frac{dq}{8\pi} e^{iqx} q \left\{ [\text{sgn}(q)]^{\delta_{\alpha\alpha'}} \tilde{\Sigma}_{\nu\nu'}^{\alpha\alpha'} + [\text{sgn}(q)]^{1-\delta_{\alpha\alpha'}} \tilde{\Delta}_{\nu\nu'}^{\alpha\alpha'} \right\}. \quad (\text{G13})$$

We observe that the spatial dependence of this correlation function stems either from the Fourier transform of $|q|$, giving rise to quasi-long-range algebraic decay $\propto 1/x^2$, or from q , which instead gives ultra-local $\partial_x \delta(x)$ behavior. We are interested only in the asymptotic tails. Thus, for $\alpha = \alpha'$, corresponding to φ - φ or θ - θ correlations, we keep only the $\tilde{\Sigma}$ -term, while for $\alpha' = \bar{\alpha} \equiv -\alpha$, corresponding to φ - θ correlations, we retain only the $\tilde{\Delta}$ -term. Using Eq. (G12) the corresponding coefficients can be expressed as

$$\tilde{\Sigma}_{\nu\nu'}^{\alpha\alpha} = \frac{1}{2} \text{tr} \left[V_+^\dagger X_{\nu\nu'} (\tau_0 + \alpha \tau_1) V_+ \right], \quad \tilde{\Delta}_{\nu\nu'}^{\alpha\bar{\alpha}} = \frac{1}{2} \text{tr} \left[V_+^\dagger (X_{\nu\nu'} \tau_3 + \alpha Y_{\nu\nu'} \tau_2) V_+ \right] = \tilde{\Delta}_{\nu'\nu}^{\bar{\alpha}\alpha}, \quad (\text{G14})$$

where we introduced the shorthand notations $X_{\nu\nu'} = |\nu\rangle\langle\nu'| + \text{h.c.}$ and $Y_{\nu\nu'} = -i(|\nu\rangle\langle\nu'| - \text{h.c.})$. We find

$$\tilde{\Sigma}_{\nu\nu}^{\alpha\alpha} = 0, \quad \tilde{\Delta}_{\nu\nu}^{\alpha\bar{\alpha}} = 0. \quad (\text{G15})$$

The first relation in Eq. (G15) implies that only φ_ν - φ_ν and θ_ν - θ_ν correlations within the same charge-spin sector exhibit algebraic tails. Similarly, the second relation means that only different charge-spin sectors produce quasi-long-range behavior in φ_ν - $\theta_{\bar{\nu}}$ cross-correlations. Before proceeding, let us outline the proof of Eq. (G15).

First, we simplify the relevant matrix elements by noting that $X_{\nu\bar{\nu}} = \sigma_1$, $X_{\nu\nu} = \sigma_0 \pm_\nu \sigma_3$ with $\pm_c = +$ and $\pm_s = -$, and $Y_{\nu\nu} = 0$. This gives

$$\tilde{\Sigma}_{\nu\bar{\nu}}^{\alpha\alpha} = \frac{1}{2} \text{tr} \left[V_+^\dagger \sigma_1 (\tau_0 + \alpha \tau_1) V_+ \right], \quad \tilde{\Delta}_{\nu\nu}^{\alpha\bar{\alpha}} = \frac{1}{2} \text{tr} \left[V_+^\dagger (\sigma_0 \pm_\nu \sigma_3) \tau_3 V_+ \right]. \quad (\text{G16})$$

We show below that the transformation V_+ can be chosen as $V_+ = \exp\{v_1\tau_1 + v_2\tau_2\}$ with $v_i = v_{i0}\sigma_0 + v_{i2}\sigma_2 + v_{i3}\sigma_3$, $v_{ij} \in \mathbb{R}$. Importantly, σ_1 does not feature in the exponent. By expanding the exponential order by order, it is straightforward to check that $V_+V_+^\dagger \in \text{span}(\sigma_{i \in \{0,2,3\}}\tau_{j \in \{1,2,3\}}, \sigma_1\tau_3)$, i.e., σ_1 and τ_3 feature only as product in $V_+V_+^\dagger$. Using cyclicity of the trace and orthogonality, $\text{tr}(\sigma_i\tau_j\sigma_{i'}\tau_{j'}) = 4\delta_{ii'}\delta_{jj'}$, this immediately implies Eq. (G15). To see why one may write V_+ in this form, first note that $V_+^\dagger\tau_3V_+ = \tau_3$ implies the general form $V_+ = \exp\{i(v_0\tau_0 + v_3\tau_3) + v_1\tau_1 + v_2\tau_2\}$, where v_i are (thus far unconstrained) hermitian 2×2 matrices. However, this parametrization is redundant: the condition $[V_+^\dagger h_{q>0} V_+]_{12} = 0$ corresponds to 8 real equations, while such V_+ has 16 real parameters. This redundancy corresponds to the freedom to perform independent unitary spin rotations in the $\tau_3 = \pm 1$ sectors, which leave $[V_+^\dagger h_{q>0} V_+]_{12} = 0$ invariant. Such a spin rotation amounts to a redefinition $V \rightarrow VU$ with $U = \exp\{i(u_0\tau_0 + u_3\tau_3)\}$, u_i hermitian. One can use this freedom to eliminate the τ_0 and τ_3 terms in the exponent of V_+ : choose $U = \exp\{-i(v_0\tau_0 + v_3\tau_3) + \dots\}$, where \dots corresponds to terms of order v^3 and higher. Applying the Baker-Campbell-Hausdorff formula to combine the exponentials of V and U , one finds that with this choice of U , only $\tau_{1,2}$ -terms appear at order v^2 , while $\tau_{0,3}$ -terms feature at order v^3 . To eliminate the latter, we include an order- v^3 counter-term in the exponent of U (entering the \dots). This term gives rise to new $\tau_{0,3}$ -terms only at order v^5 , which, together with $\tau_{0,3}$ -terms at order v^5 originating from the leading term in the exponent of U , can be accounted for by a v^5 -contribution to the exponent of U . In this way, one can eliminate $\tau_{0,3}$ -terms in V_+ . This shows that one can choose

$$V_+ = \exp\{v_1\tau_1 + v_2\tau_2\}. \quad (\text{G17})$$

It remains to show that $\text{tr}(v_{1,2}\sigma_1) = 0$. To this end, consider $V_+^\dagger h_{q>0} V_+$ to leading order in v and demand that the Nambu-12 block vanishes. This gives $(h + \{v_1\tau_1 + v_2\tau_2, h\})_{12} = 0$. Multiplying this equation by σ_1 and taking the trace gives $\sum_\nu \frac{|\omega_{\nu,q}|}{2} (e^{i\eta_{\nu,q}} + 1)(v_{11} - iv_{21}) = 0$, which can only be satisfied if $v_{11} = v_{21} = 0$. It is straightforward to check that this pattern persists to higher orders.

In the end, Eq. (G13) simplifies to

$$F_{\nu\nu'}^{\alpha\alpha}(x) = -\frac{1}{4\pi x^2} \left| \tilde{k}_\nu \tilde{k}_{\nu'} \right|^{-\frac{\alpha}{4}} \tilde{\Sigma}_{\nu\nu'}^{\alpha\alpha} + \dots, \quad F_{\nu\nu'}^{\alpha\bar{\alpha}}(x) = -\frac{1}{4\pi x^2} \left| \frac{\tilde{k}_\nu}{\tilde{k}_{\nu'}} \right|^{-\frac{\alpha}{4}} \tilde{\Delta}_{\nu\nu'}^{\alpha\bar{\alpha}} + \dots, \quad (\text{G18})$$

where the ellipses denote short-range terms neglected below. Collecting the above results, at the $\lambda \rightarrow 0$ fixed point, the equal-time steady-state correlation functions $C_{AB}(x)$ in Eq. (G7) are given by Eq. (15), involving only the six real-valued coefficients ($\nu = c, s$)

$$\Sigma_\nu^+ = \frac{1}{2\pi^2} |\tilde{k}_\nu|^{-\frac{1}{2}} \tilde{\Sigma}_{\nu\nu}^{++}, \quad \Delta_{\nu\bar{\nu}} = -\frac{1}{2\pi^2} |\tilde{k}_{\bar{\nu}}/\tilde{k}_\nu|^{\frac{1}{4}} \tilde{\Delta}_{\nu\bar{\nu}}^{+-} + \kappa \Sigma_\nu^+, \quad \Sigma_\nu^- = \frac{1}{2\pi^2} |\tilde{k}_\nu|^{\frac{1}{2}} \tilde{\Sigma}_{\nu\nu}^{--} + 2\kappa \Delta_{\bar{\nu}\nu} - \kappa^2 \Sigma_\nu^+. \quad (\text{G19})$$

To obtain their values as shown in Fig. 2 of the main text, we have numerically determined the transformation V_+ .

2. Strong-coupling fixed point

We next consider the massive case $m_\lambda \neq 0$ in Eq. (G2), where a Gaussian fixed point describes the strong-coupling limit $|\lambda| \rightarrow \infty$. As opposed to the massless case, the transformation V_q now also depends on the magnitude of q , making it slightly more cumbersome to find the spatial asymptotics of $F_{\nu\nu'}^{\alpha\alpha'}(x)$. We can make analytical progress by treating the κ term perturbatively. To this end, we first find rotations $V_{\nu,q}$ that bring $h_{\nu,q}$ into lower triangular form. It is straightforward to see that this is achieved by the Bogoliubov transformation $V_{\nu,q} = \exp\{v_{\nu,q}\tau_2\}$ with $v_{\nu,q}$ defined by

$$\sinh(2v_{\nu,q}) = \frac{\text{Im}(\omega_{\nu,q})}{\text{Re}(\omega_{\nu,q})}, \quad \tilde{h}_{\nu,q} \equiv V_{\nu,q}^\dagger h_{\nu,q} V_{\nu,q} = \omega_{\nu,q}\tau_0 + |\omega_{\nu,q}|(e^{i\eta_{\nu,q}} - 1)\tau_-. \quad (\text{G20})$$

Applying $V_q^{(0)} = \text{diag}(V_{c,q}, V_{s,q})$ to h_q brings the first term in Eq. (G3) into lower triangular form, leaving only a contribution due to the κ -term,

$$\left[(V_q^{(0)})^\dagger h_q V_q^{(0)} \right]_{12} = v_F q \sigma_2 [-\kappa_+ \sinh(v_{c,q} - v_{s,q}) + i\kappa_- \cosh(v_{c,q} + v_{s,q})]. \quad (\text{G21})$$

We next apply a second Bogoliubov transformation W_q close to unity that eliminates the κ -term in the Nambu-12 block to leading order. Explicitly, we demand

$$[W_q^\dagger \text{diag}(\tilde{h}_{c,q}, \tilde{h}_{s,q}) W_q]_{12} = - \left[(V_q^{(0)})^\dagger h_q V_q^{(0)} \right]_{12}. \quad (\text{G22})$$

This is achieved by [62] $W = 1 + (w_1\tau_1 + w_2\tau_2)\sigma_2$, with the coefficients

$$\begin{aligned} w_1 &= \frac{v_F q}{|\sum_\nu \omega_\nu|^2} \sum_\nu [\kappa_+ \sinh(v_{c,q} - v_{s,q}) \operatorname{Re}(\omega_\nu) - \kappa_- \cosh(v_{c,q} + v_{s,q}) \operatorname{Im}(\omega_\nu)], \\ w_2 &= \frac{v_F q}{|\sum_\nu \omega_\nu|^2} \sum_\nu [\kappa_+ \sinh(v_{c,q} - v_{s,q}) \operatorname{Im}(\omega_\nu) + \kappa_- \cosh(v_{c,q} + v_{s,q}) \operatorname{Re}(\omega_\nu)]. \end{aligned} \quad (\text{G23})$$

Consider now the correlation functions in Eq. (G9). To proceed, we use the approximate expression $V_q \simeq V_q^{(0)} W_q$, giving

$$\operatorname{tr} \left(V_q^\dagger M_{\nu\nu'}^{\alpha\alpha'} V_q \right) \simeq \operatorname{tr} \left((V_q^{(0)})^\dagger M_{\nu\nu'}^{\alpha\alpha'} V_q^{(0)} \right) + \operatorname{tr} \left(\left\{ (w_1\tau_1 + w_2\tau_2)\sigma_2, (V_q^{(0)})^\dagger M_{\nu\nu'}^{\alpha\alpha'} V_q^{(0)} \right\} \right). \quad (\text{G24})$$

We derive first the correlations originating from the first term. $V_q^{(0)}$ does not mix charge and spin sectors, and thus at this order there are no such cross-correlations. Explicitly,

$$F_{\nu\nu'}^{\alpha\alpha'}(x) \Big|^{(0)} \equiv \int \frac{dq}{8\pi} e^{iqx} q \left(\frac{v_F q}{|\omega_{\nu,q}|} \right)^{\frac{\alpha}{2}} \left(\frac{v_F q}{|\omega_{\nu',q}|} \right)^{\frac{\alpha'}{2}} \left\{ \operatorname{tr} \left((V_q^{(0)})^\dagger M_{\nu\nu'}^{\alpha\alpha'} V_q^{(0)} \right) - 2\delta_{\nu\nu'}(1 - \delta_{\alpha\alpha'}) \right\} \quad (\text{G25})$$

$$= \delta_{\nu\nu'} \int \frac{dq}{8\pi} e^{iqx} q \left(\frac{v_F q}{|\omega_{\nu,q}|} \right)^{\frac{\alpha+\alpha'}{2}} \left\{ \operatorname{tr} \left((V_q^{(0)})^\dagger M_{\nu\nu}^{\alpha\alpha'} V_q^{(0)} \right) - 2(1 - \delta_{\alpha\alpha'}) \right\} \quad (\text{G26})$$

For $\alpha' = -\alpha$, this gives ultra-short range behavior,

$$F_{\nu\nu}^{\alpha\bar{\alpha}}(x) \Big|^{(0)} = \int \frac{dq}{8\pi} e^{iqx} q \left\{ \operatorname{tr} \left(V_{\nu,q}^\dagger (\tau_3 - i\alpha\tau_2) V_{\nu,q} \right) - 2 \right\} \propto \partial_x \delta(x). \quad (\text{G27})$$

For $\alpha' = \alpha$, one instead finds

$$F_{\nu\nu}^{\alpha\alpha}(x) \Big|^{(0)} = \int \frac{dq}{8\pi} e^{iqx} q \left(\frac{v_F q}{|\omega_{\nu,q}|} \right)^\alpha \operatorname{tr} \left(V_{\nu,q}^\dagger (\tau_0 + \alpha\tau_1) V_{\nu,q} \right) = \int \frac{dq}{4\pi} e^{iqx} q \left(\frac{v_F q}{|\omega_{\nu,q}|} \right)^\alpha \frac{|\omega_{\nu,q}|}{\operatorname{Re}(\omega_{\nu,q})}. \quad (\text{G28})$$

The behavior of $F_{\nu\nu}^{\alpha\alpha}(x)$ at large $|x|$ is controlled by the branch points of the integrand which occur at $v_F q \in \left\{ \pm \sqrt{\frac{im_\lambda^2}{k_\nu}}, \pm \sqrt{\frac{-i(m_\lambda^*)^2}{k_\nu^*}} \right\}$, leading to an exponential decay,

$$F_{\nu\nu}^{\alpha\alpha}(x) \Big|^{(0)} = \frac{f_\nu^\alpha(x)}{(|x|/\xi_\nu)^{3/2}} e^{-|x|/\xi_\nu}, \quad \xi_\nu = v_F \left| \operatorname{Im} \left(\sqrt{\frac{im_\lambda^2}{k_\nu}} \right) \right|^{-1}, \quad (\text{G29})$$

where the α -dependent prefactor $f_\nu^\alpha(x)$ oscillates on a scale set by the wavevector $|\operatorname{Re}(\sqrt{im_\lambda^2/k_\nu})|/v_F$.

Next, we analyze which of the thus far vanishing correlations become finite when the leading correction due to the κ -term is included. As $\ln W$ is off-diagonal in charge-spin space, see Eq. (G24), it is clear that only $\nu' = -\nu$ correlations receive a contribution. The set of branch points now involves the branch points due to $\omega_{c,q}$ and $\omega_{s,q}$. The decay is set by the point closest to the real axis, resulting in $F_{\nu\nu'}^{\alpha\alpha'} \sim \kappa e^{-|x|/\xi_{cs}}$ with $\xi_{cs} = \max\{\xi_c, \xi_s\}$. To conclude, in this phase we find short-ranged correlations, where the length scale governing the exponential decay is described by Eq. (16).